Core-collapse supernovae in dense environments

Particle acceleration and non-thermal emission

Robert Brose, Jonathan Mackey, Iurii Sushch

HONEST workshop on PeVatrons, 29 November 2022

Online

Galactic cosmic-rays

Possible sources

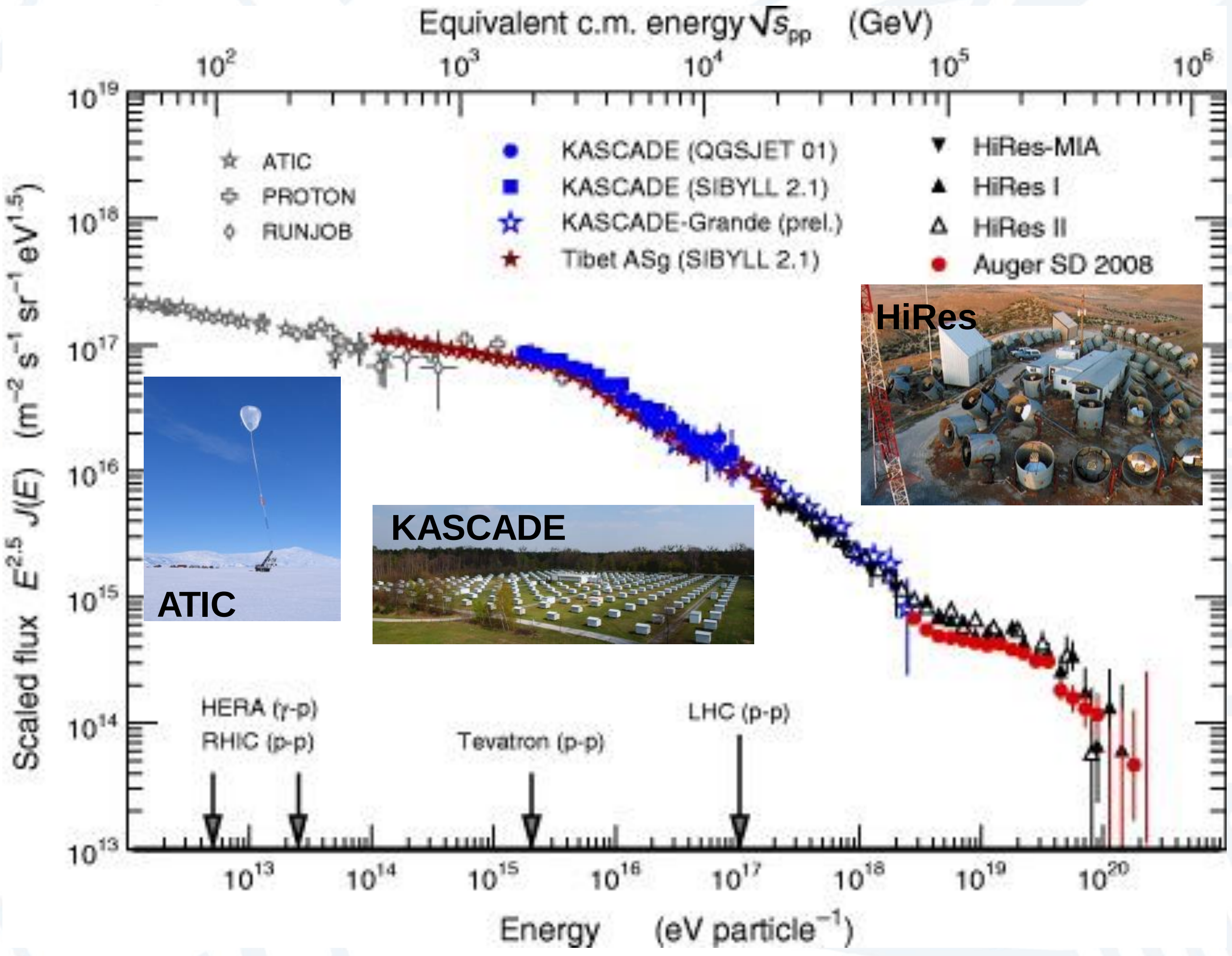

Figure: The cosmic ray spectrum (Blümer et al. 2019)

DIAS
Institiúid Ard-Léinn Bhaile Átha Cliath | Dublin Institute for Advanced Studies

Sources of Galactic CRs?

Supernova remnants?

Galactic cosmic-rays

Possible sources

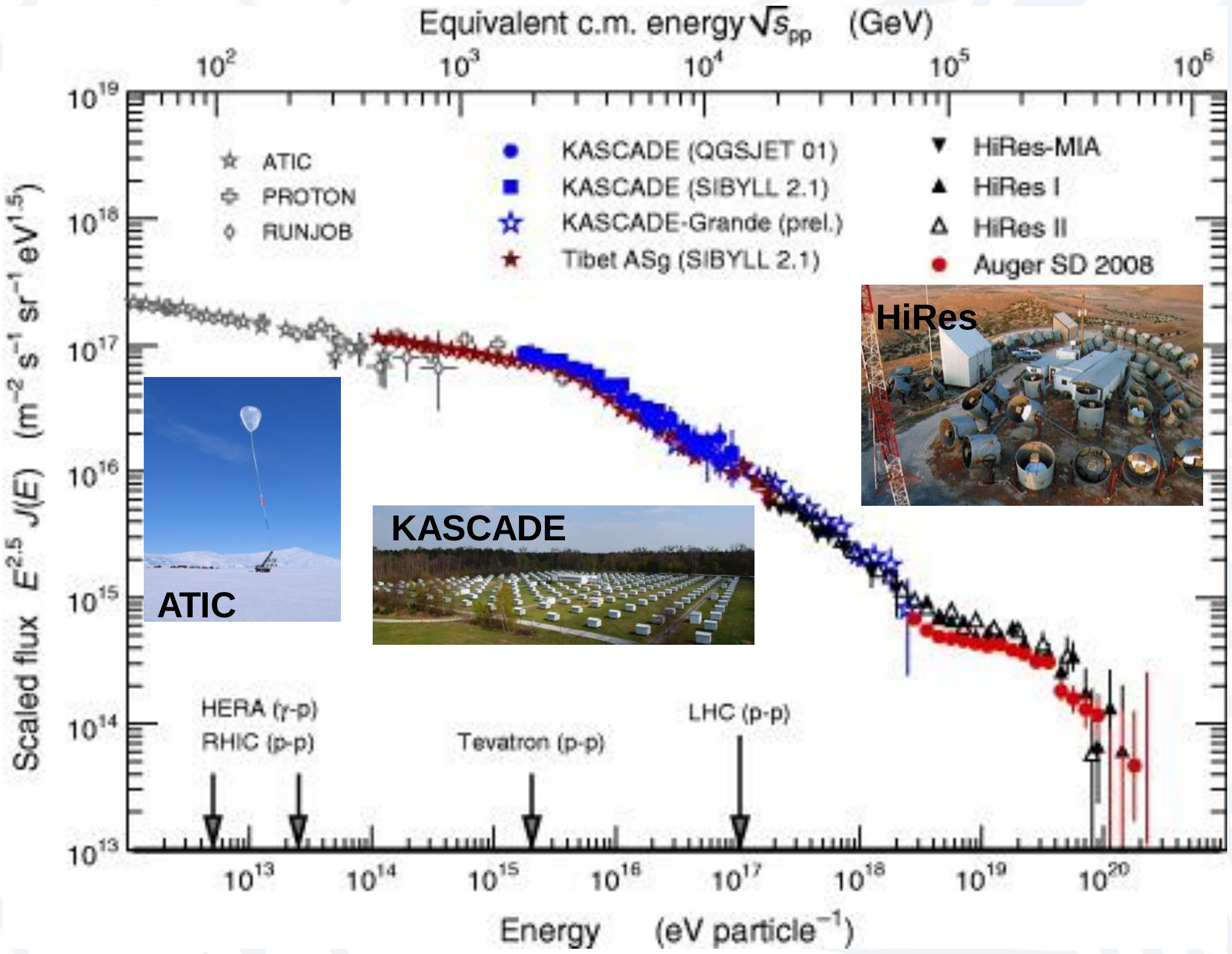

Figure: The cosmic ray spectrum (Blümer et al. 2019)

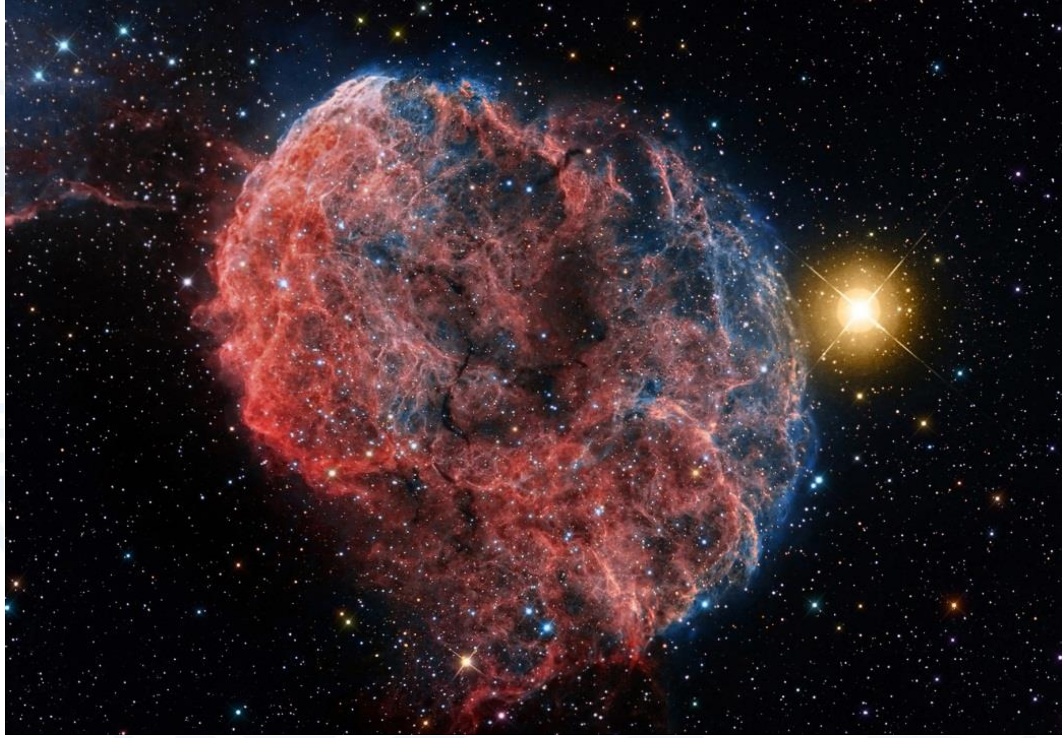

Figure: IC443 – multi wavelength image (credit: Dieter Willasch)

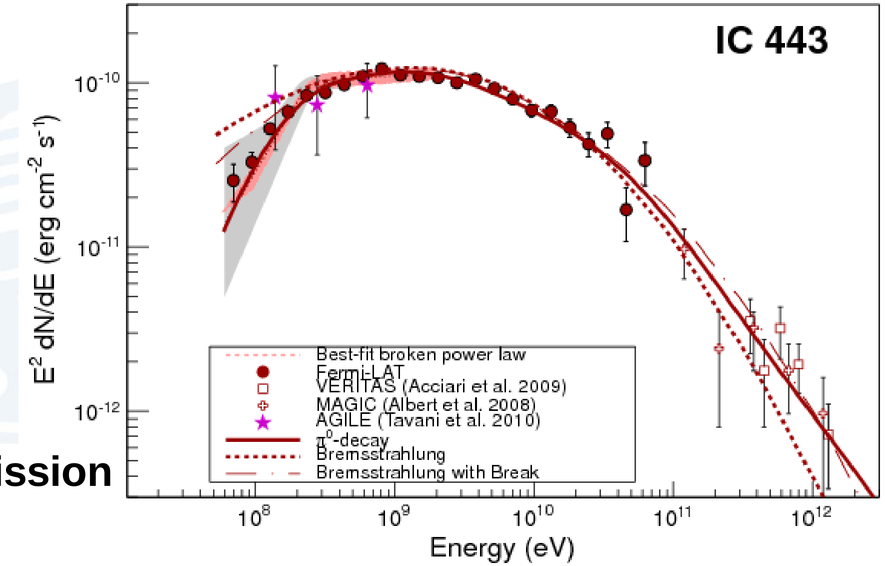

Figure: IC443 – gamma ray emission (Funk et al. 2013)

Galactic cosmic-rays

Possible sources

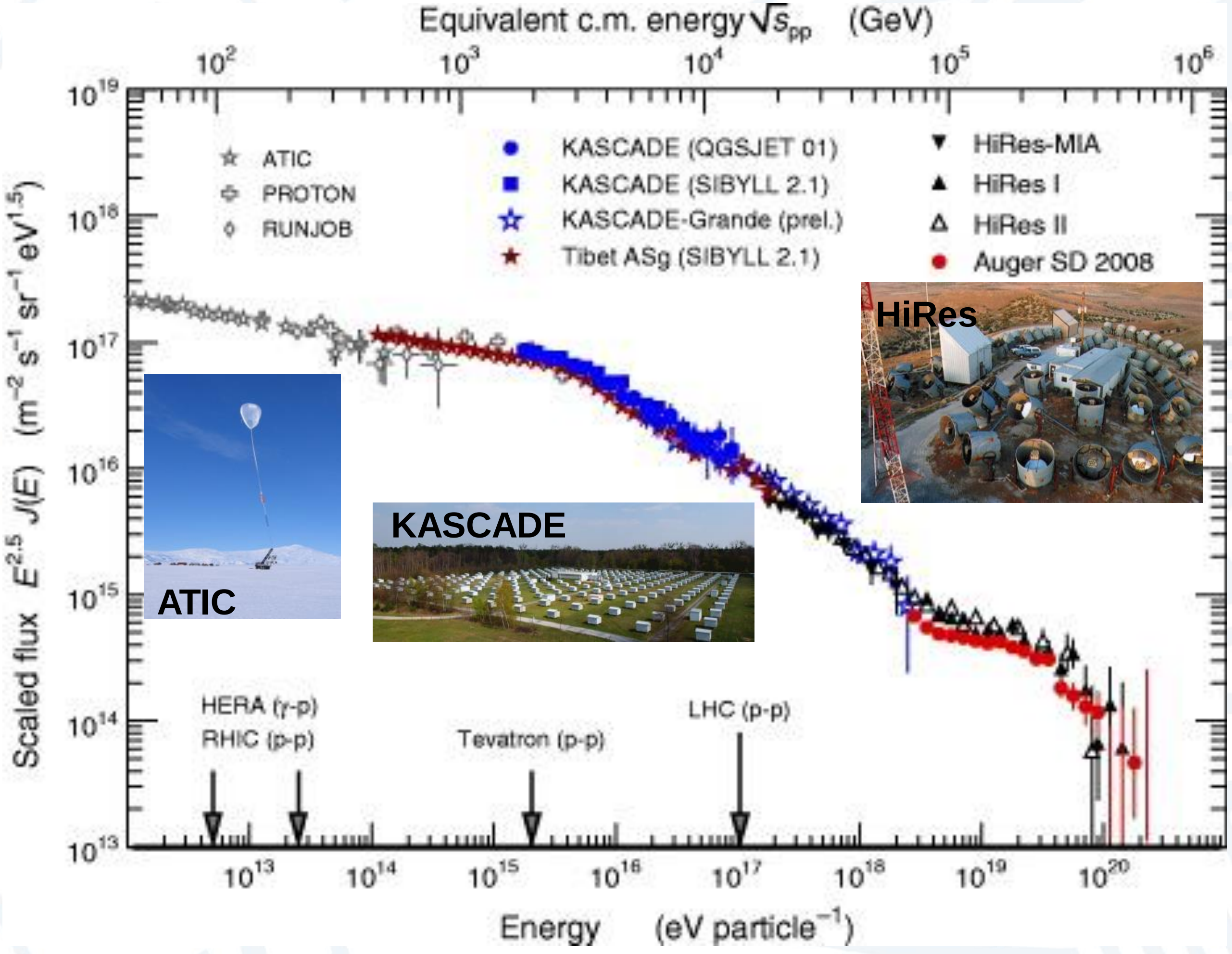

Figure: The cosmic ray spectrum (Blümer et al. 2019)

Figure: Cas A, (credit: Chandra, NASA/CXC/SAO)

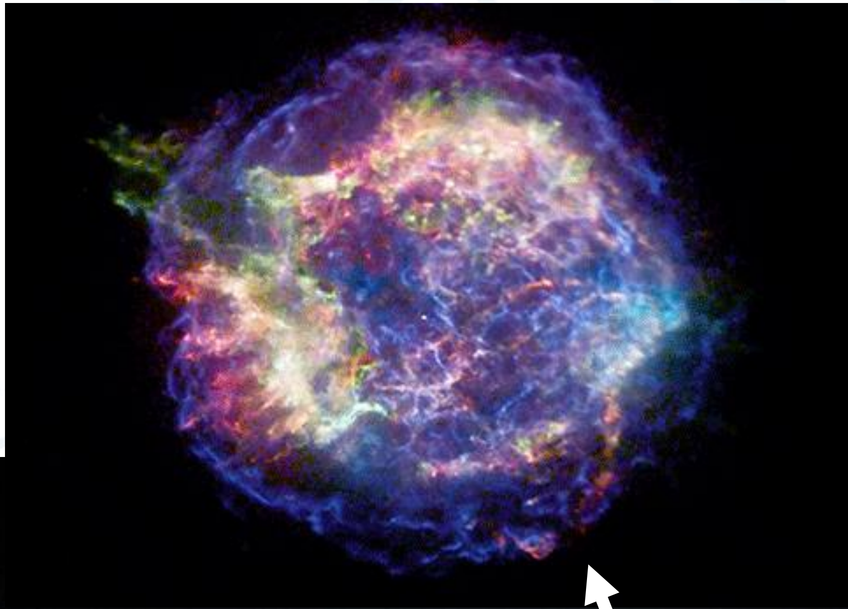

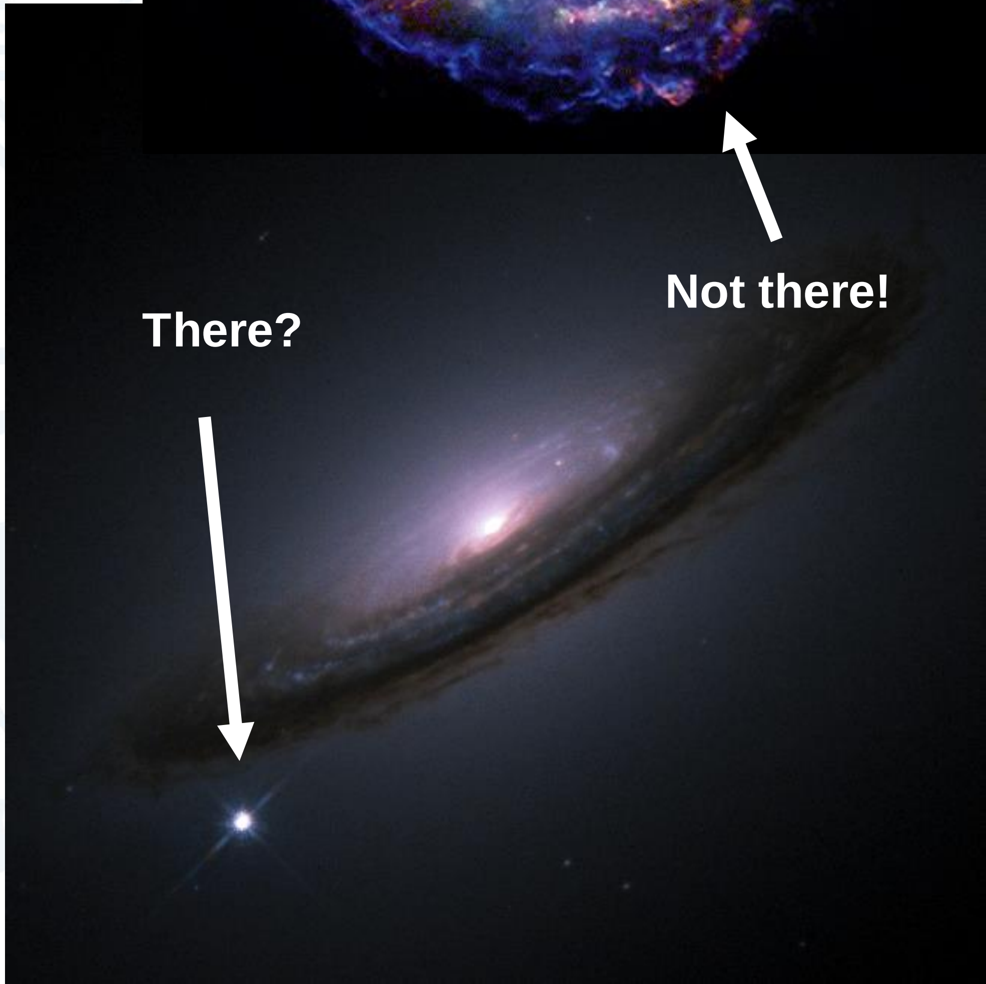

Figure: SN1994D (credit: Hubble, NASA/ESA)

SNRs as cosmic-ray sources

Where to look

- High magnetic fields required → Self-consistent amplification:

$$\Gamma_{\delta B} \propto \partial N_{CR}/\partial r \propto \rho_{CSM}$$

→ Progenitor stars with extreme mass-loss:
RSGs ←→ Type-IIP SNe (not today)
LBVs ←→ Type-IIn SNe

- Type-IIn SNe: Radio bright even after years and signs of CSM-interaction

- Theoretical models predict high-energy radiation if particle acceleration is efficient (e.g., Murase+2011, Marcowith+2018);
but only smooth winds so far

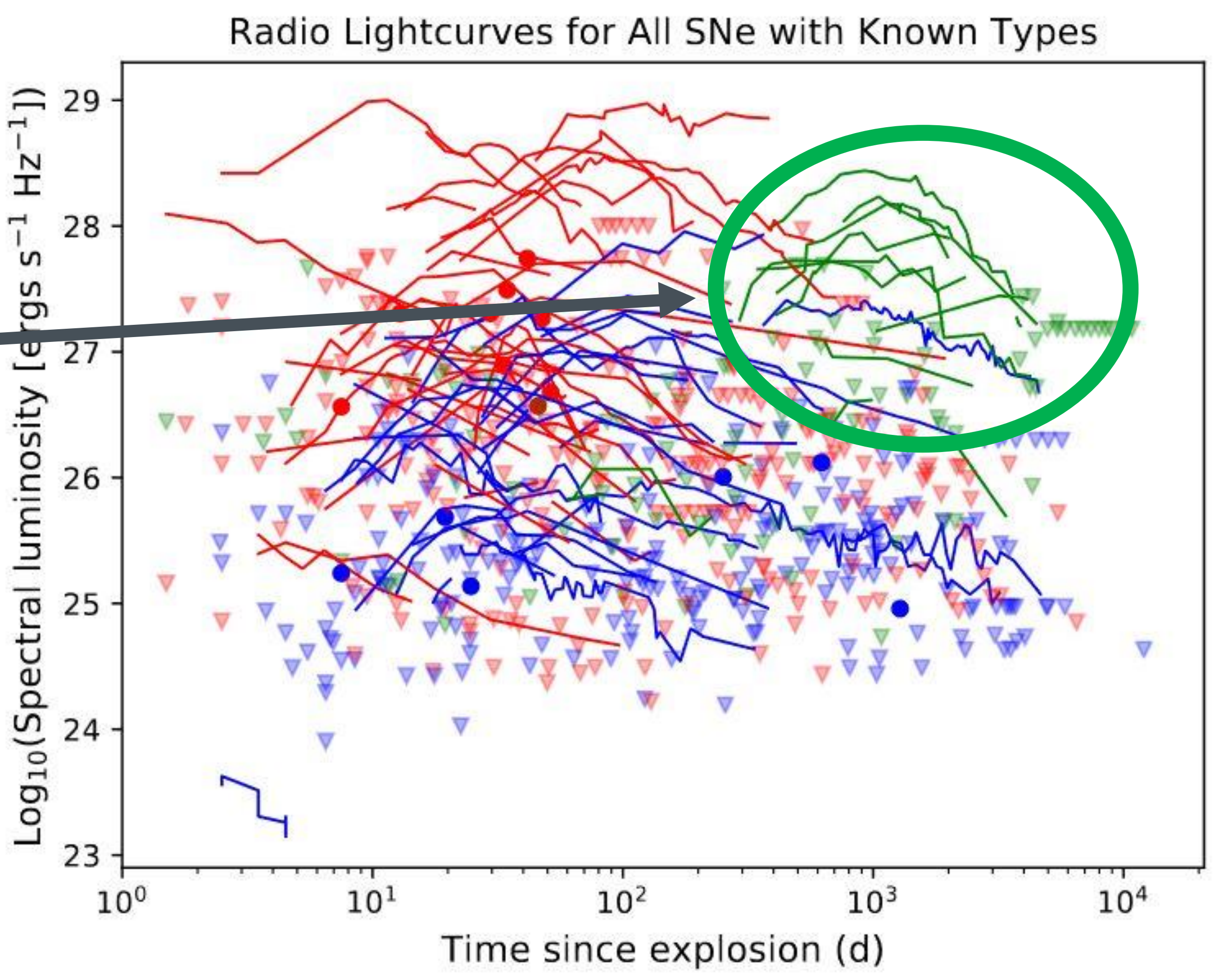

Figure: **Early-time Radio emission from SNs of various types (Bietenholz et al.2021)**

SNRs as cosmic-ray sources

Experimental evidence

- H.E.S.S. Collaboration (2019) obtained upper limits on TeV emission from nearby CCSNe
- Ongoing HESS ToO programme so far has no detections
- Xi+(2020) detected γ-rays from the location of SN 2004dj, a bright and nearby SN IIP, with FERMI-LAT
- A recent variability analysis of FERMI-LAT data found evidence in support of 2 further detections (Prokhorov+2021).
- Also suggestion of increasing flux from SN1987A with FERMI-LAT (Malyshev+2019)

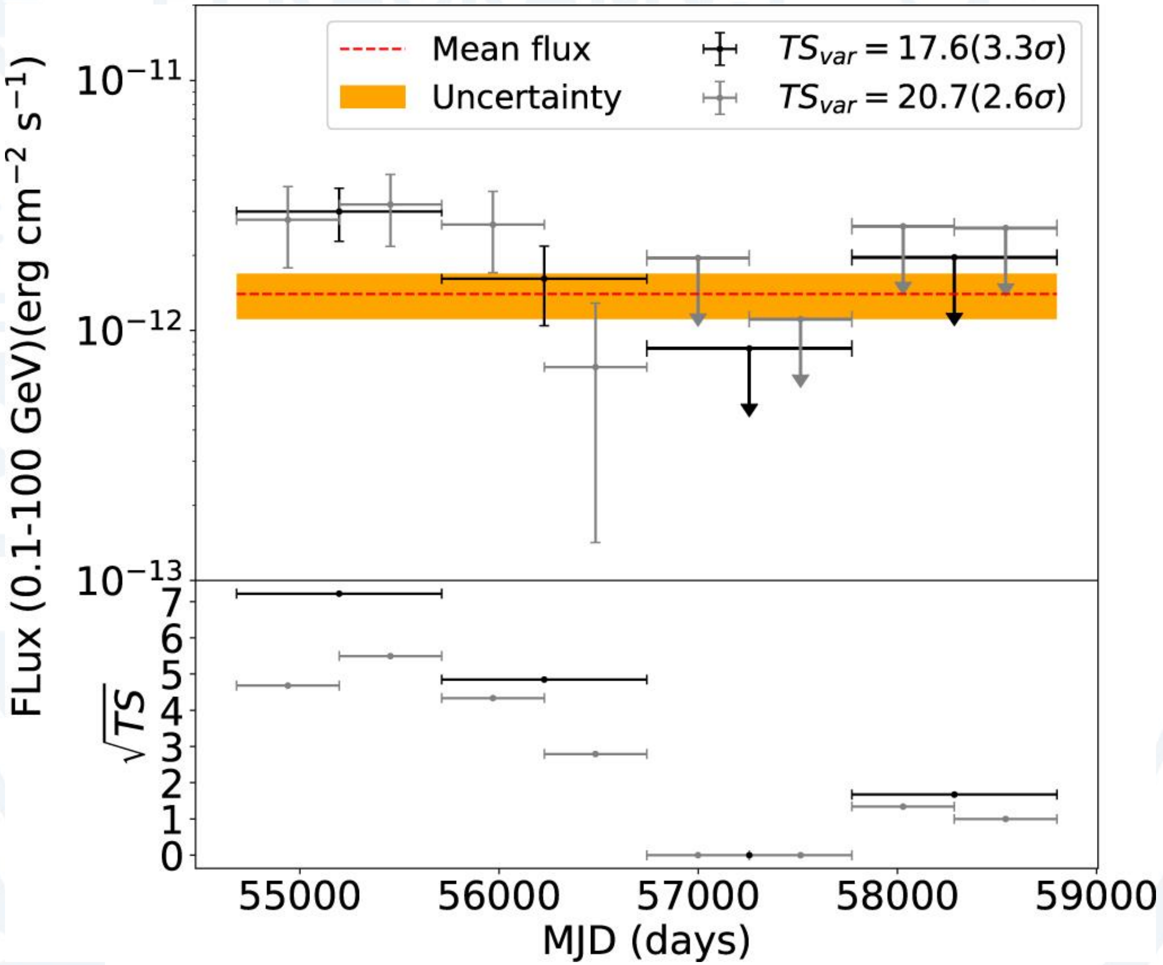

Figure: Light curve of the gamma-ray flux from SN 2004dj (Xi et al. 2020)

Fermi acceleration

Coupled equations

DIAS

Institiúid Ard-Léinn Bhaile Átha Cliath | Dublin Institute for Advanced Studies

Powered by RATPAC

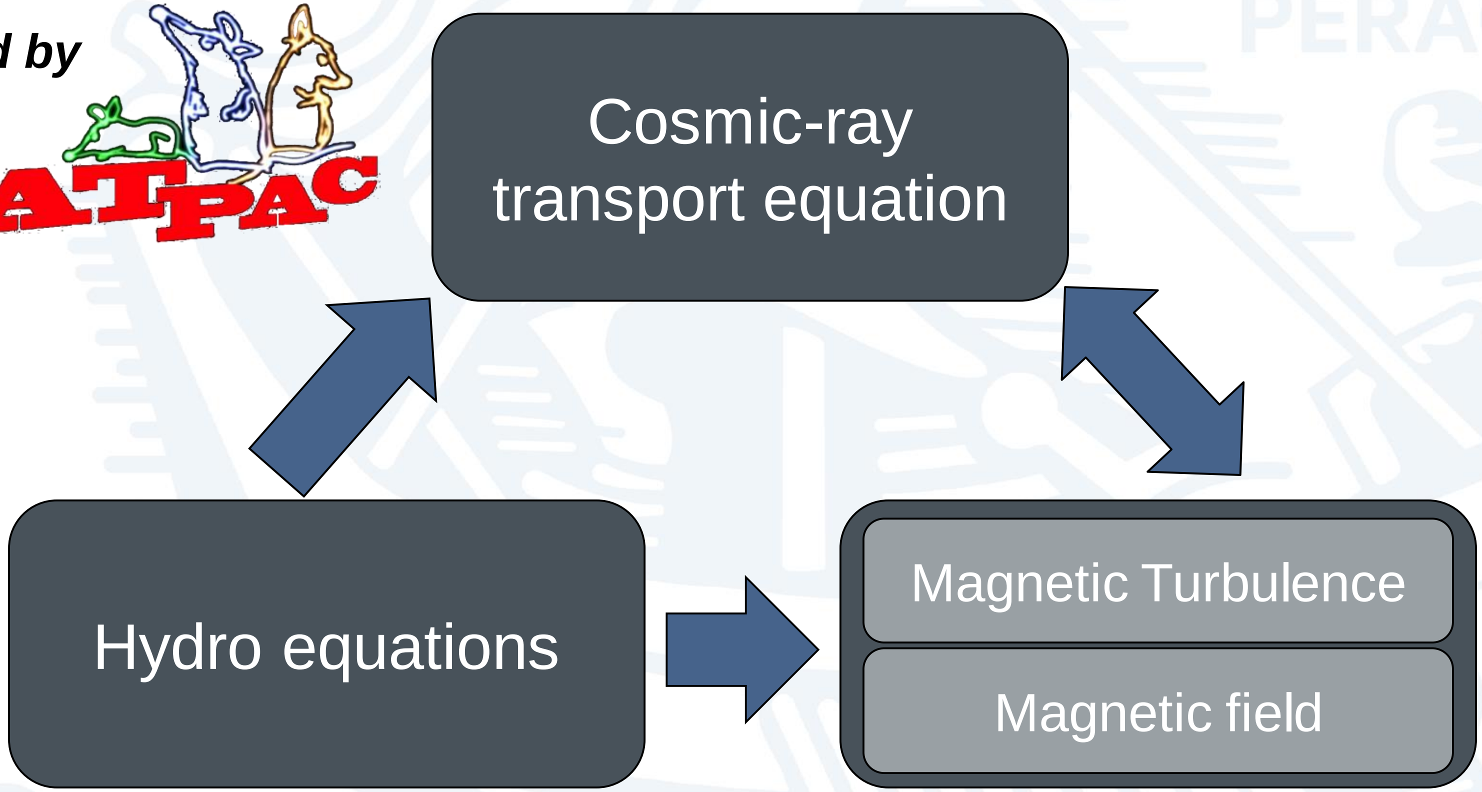

Well-tested code in development since 2012

- 10+ papers
- 140+ citations

Standard DSA

Fermi acceleration

The equations

$$\frac{\partial N}{\partial t} = \underbrace{\nabla D_r \nabla N}_{\text{Diffusion}} - \underbrace{\nabla v N}_{\text{Advection}} - \frac{\partial}{\partial p}\left(\underbrace{N\dot{p}}_{\text{Cooling}} - \underbrace{\frac{v}{3}Np}_{\text{Acceleration}}\right) + \underbrace{Q}_{\text{Injection}}$$

$$\frac{\partial E_W}{\partial t} = -\underbrace{\left(v\nabla_r E_W + c\nabla_r v E_W\right)}_{\text{Advection + Compression}} + \underbrace{k^3 \nabla_k D_k \nabla_k \frac{E_W}{k^3}}_{\text{Cascading}} + \underbrace{2\left(\Gamma_g - \Gamma_d\right)E_W}_{\text{Growth + Damping}}$$

$$\frac{\partial}{\partial t}\begin{pmatrix} \varrho \\ \boldsymbol{m} \\ E \end{pmatrix} + \nabla \begin{pmatrix} \varrho \boldsymbol{v} \\ \boldsymbol{m}\boldsymbol{v} + (P)\boldsymbol{I} \\ (E+P)\boldsymbol{v} \end{pmatrix} = \begin{pmatrix} 0 \\ 0 \\ L \end{pmatrix}$$

$$\frac{\rho v^2}{2} + \frac{P}{\gamma - 1} = E$$

The equations are solved:

- One dimensional
- Spherically symmetric
- Monoenergetic injection
- Including Synchrotron and inverse-Compton cooling for electrons
- On a comoving, expanding grid for turbulence and CRs → no free escape boundary

Fermi acceleration

Turbulence setup

Initial turbulence derived from 1/10th of the Galactic diffusion coefficient

$$D_r(t=0) = 10^{28}\left(\frac{pc}{10GeV}\right)^{1/3}\left(\frac{B_0}{3\mu G}\right)^{-1/3} cm^2/s$$

Growth rate based on pressure gradient of CRs (resonant CR-instability *x*10)

$$\Gamma_r = \mathbf{10}\,\frac{v_A p^2 v}{3E_W}\left|\frac{\partial N}{\partial r}\right|$$

Damping as diffusion in wavenumber space

$$\mathrm{D}_k = k^3 v_A \sqrt{\frac{E_W}{2B_0^2}}$$

Hydrodynamic Setup

SNe expanding into a steady wind medium

DIAS

"Luminous Blue Variable (LBV)" model (Brose et al. 2022)

- Dense and powerful wind from a massive star
- $\dot{M} = 10^{-2} M_{\odot}/yr; 3 \cdot 10^{-4} M_{\odot}/yr$
- $v_{\infty} = 100\ km/s$

- Model 1: fixed **5μG** magnetic field in the wind at all radii
- Model 2: ***1 G* at 1000 Rsun** stellar field with $B \propto r^{-1}$ at large r
- $E = 10^{51} erg,\ \ M_{ej} = 10 M_{\odot}$, density power-law index $n = 10$, Initial ejecta-radius: $10^{14}\ cm$.

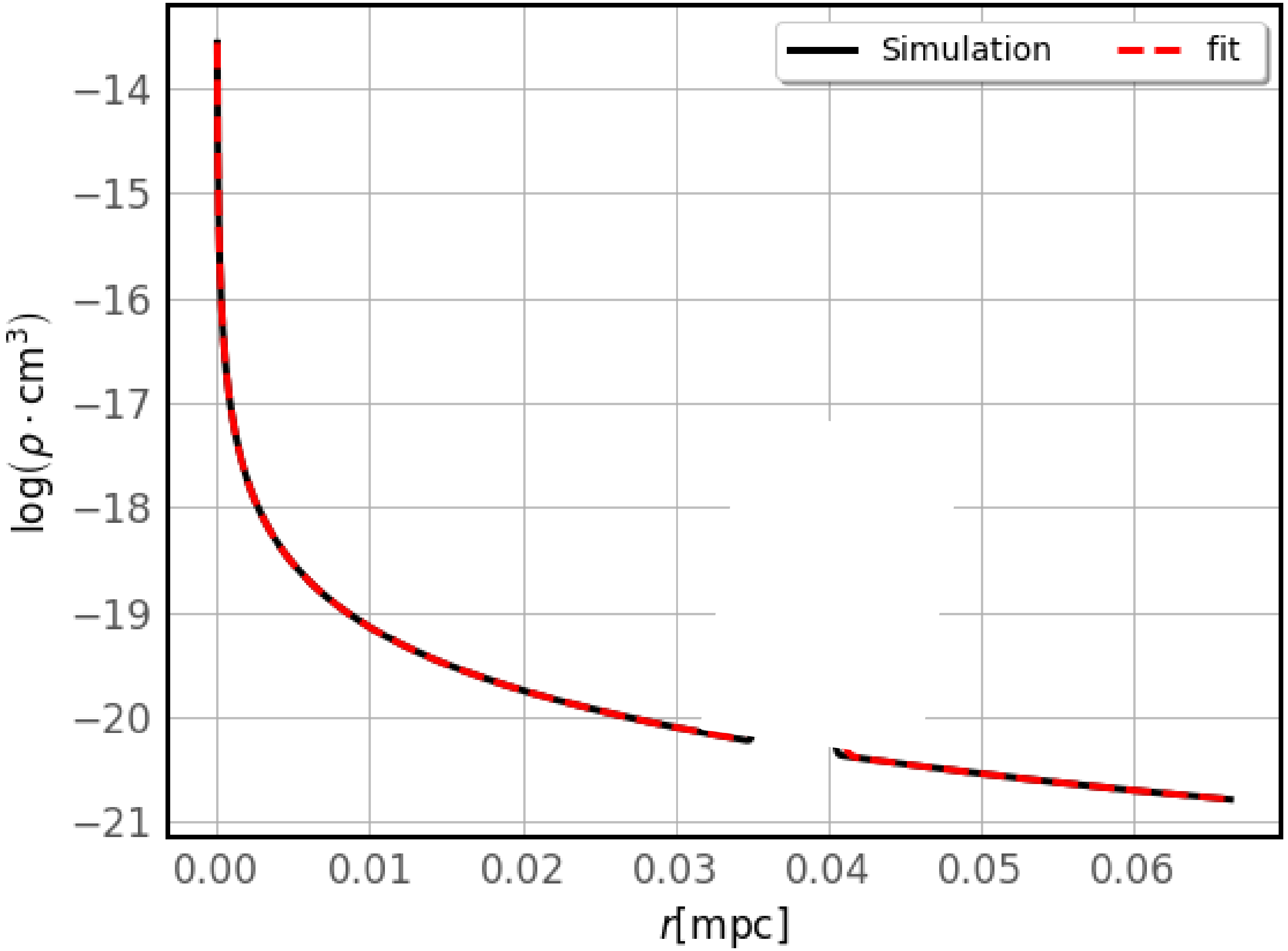

Figure: CSM-structure for a LBV with a smooth wind (example plot)

Non-thermal particle distribution

Interaction with inhomogeneous media: LBV

DIAS

- Adding a (gaussian) CSM-shell with:

$$M_{shell} = 2M_{\odot}$$
$$R_{shell} \approx 30\text{mpc}$$
$$D_{shell} \approx 1\text{mpc}$$

- Modest steady mass-loss with:

$$\dot{M} = 10^{-4} M_{\odot}/\text{yr}$$

- Shock-shell interaction after

$$\approx 100\text{days}$$

- Interaction triggers reflected shocks – shock-shock interactions after:

$$\approx 124\text{days} + \approx 2.8\text{yrs}$$

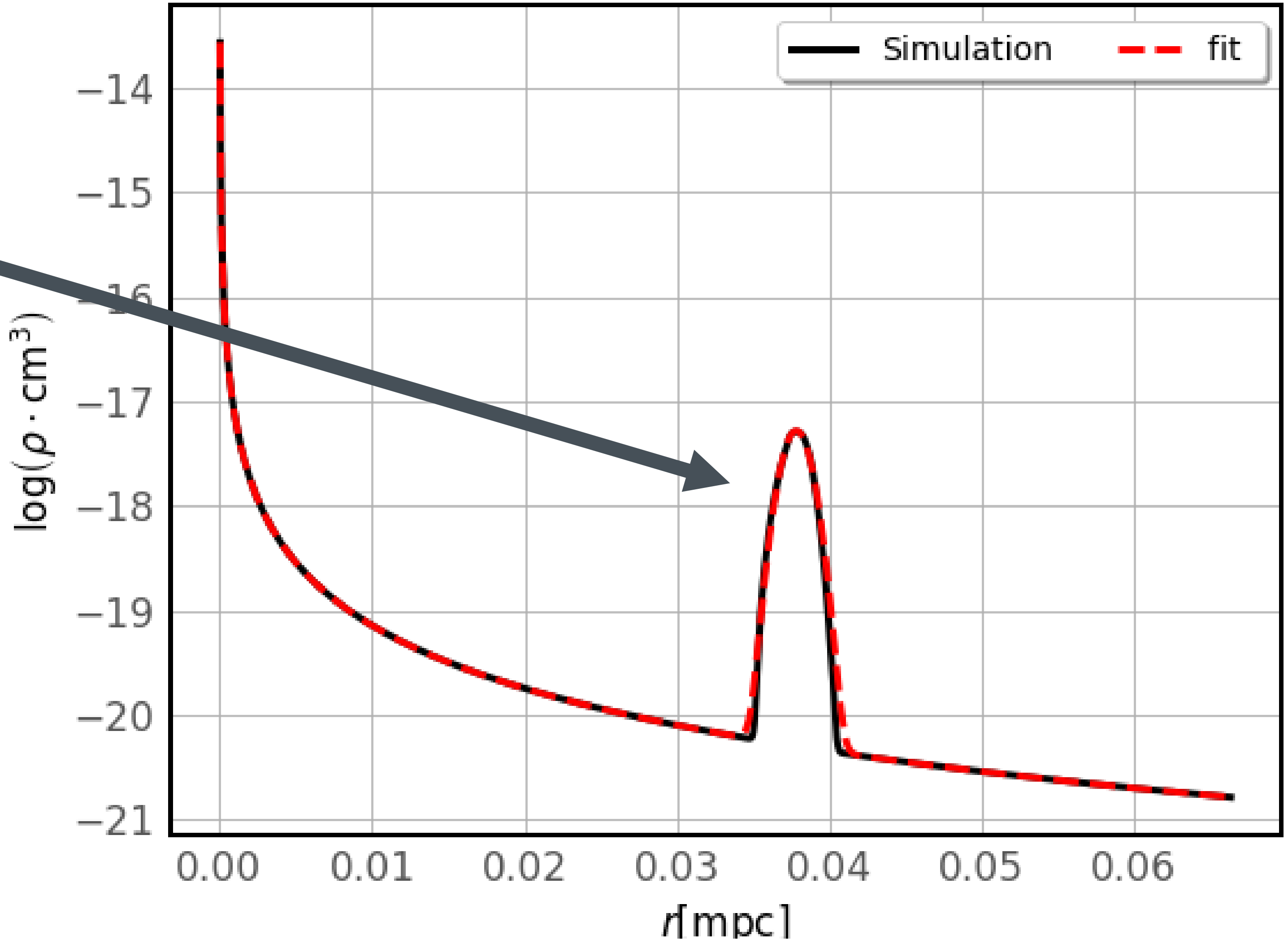

Figure: CSM-structure for a LBV with a episode of high mass-loss in the past (example plot)

Results

Thermal X-ray emission
Model vs. measurement

Smooth wind:

- Continuum X-ray emission from post-shock medium
- X-ray absorption by traces of heavy elements → only relevant for very-high mass-loss rates (dashed vs. solid blue)

Shell:

- Peak-luminosity consistent with observational values
- Shock-shock interaction might cause additional rebrightening-features

Figure: X-ray luminosity over time.

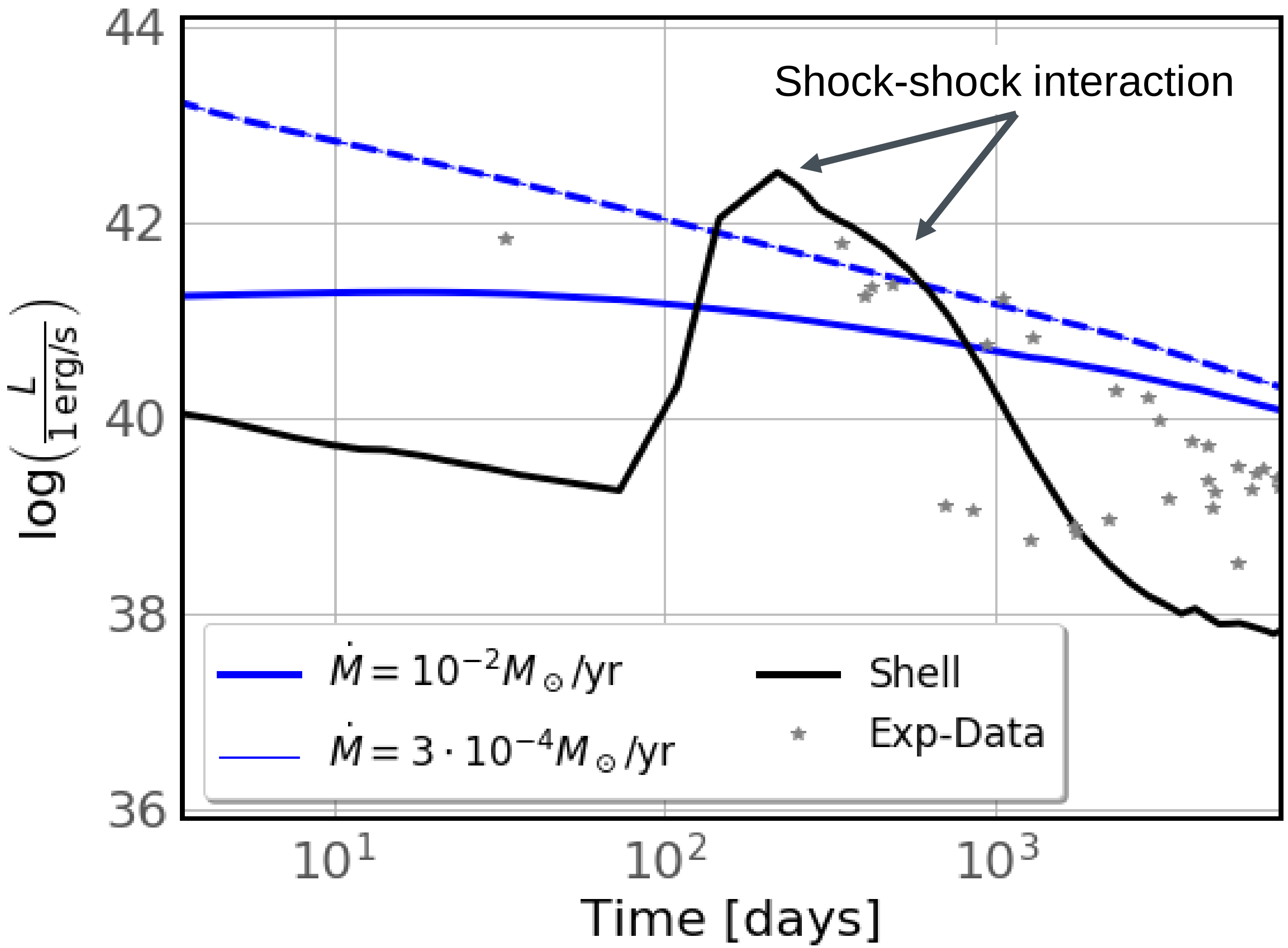

Non-thermal particle distribution
Time evolution of the maximum energy

DIAS

- Fit spectrum with power-law plus exponential cutoff → E_{max}
- **Acceleration time** is **~1 month** to get to quasi-steady state

Smooth wind:

- $E_{max} \approx 700$ TeV for LBV (high $\dot{M}$, $B \propto r^{-1}$) (stellar field is already quite strong)

Shell:

- Shock-shell interaction reduces E_{max} of freshly accelerated CRs
- Reaccelerated shock after shell passage propagates into amplified field of previously escaped CRs → Boost to E_{max}

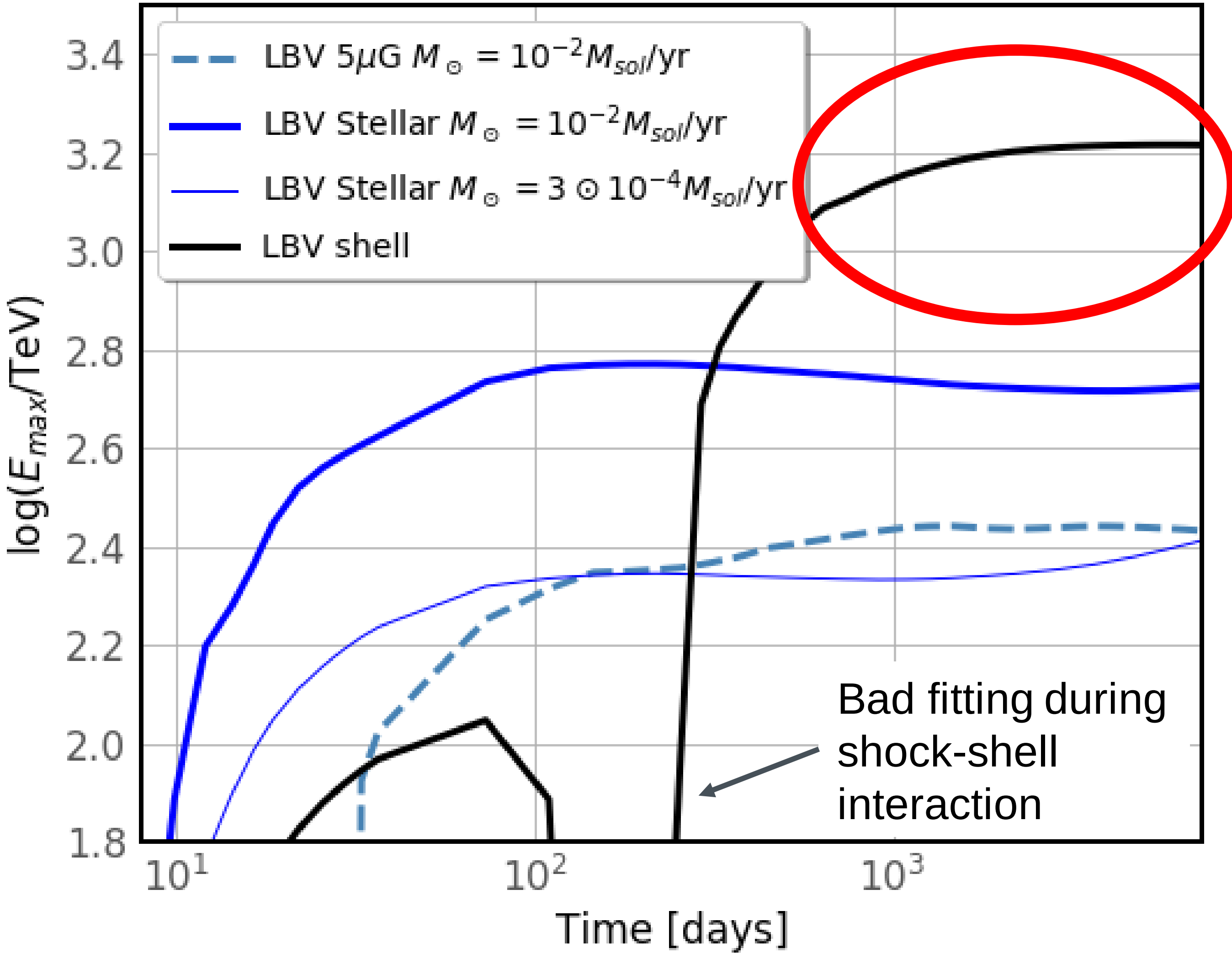

Figure: Maximum energy over time.

Non-thermal particle distribution

Time evolution of the maximum energy

DIAS

E_{max} is boosted by shell-interaction

$$E_{max} \geq 1PeV$$

- The earlier the interaction with the shell, the higher the maximum energy
- E_{max} > 1PeV if interaction before ~100days

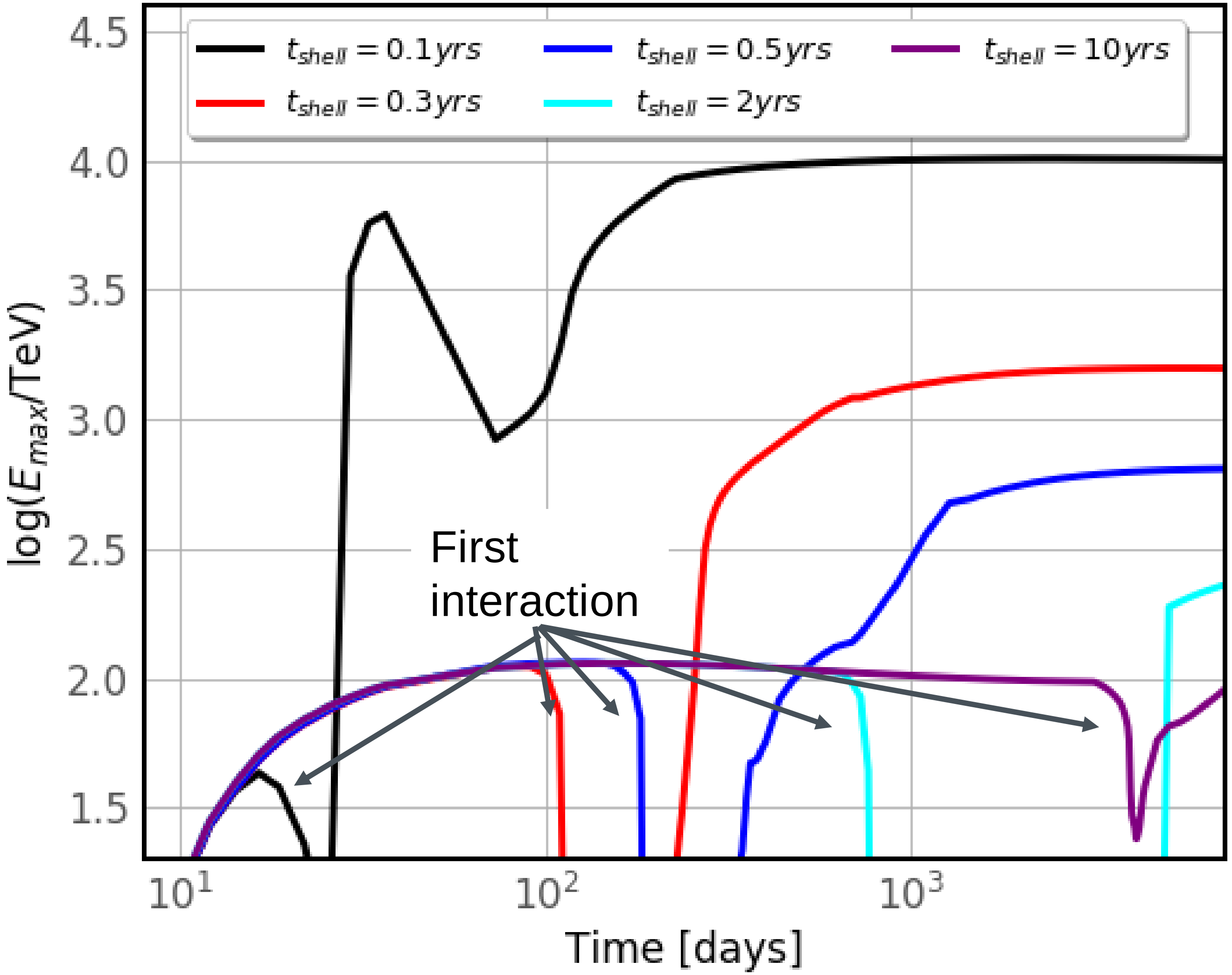

Figure: Maximum energy over time.

Gamma-ray emission

Time evolution of gamma-ray emission

- Gamma-gamma absorption (SN-photosphere): Strong attenuation in the TeV-range

- **Fluxes well below experimental upper-limits even for extreme mass loss**

Figure: Gamma-ray luminosity over time.

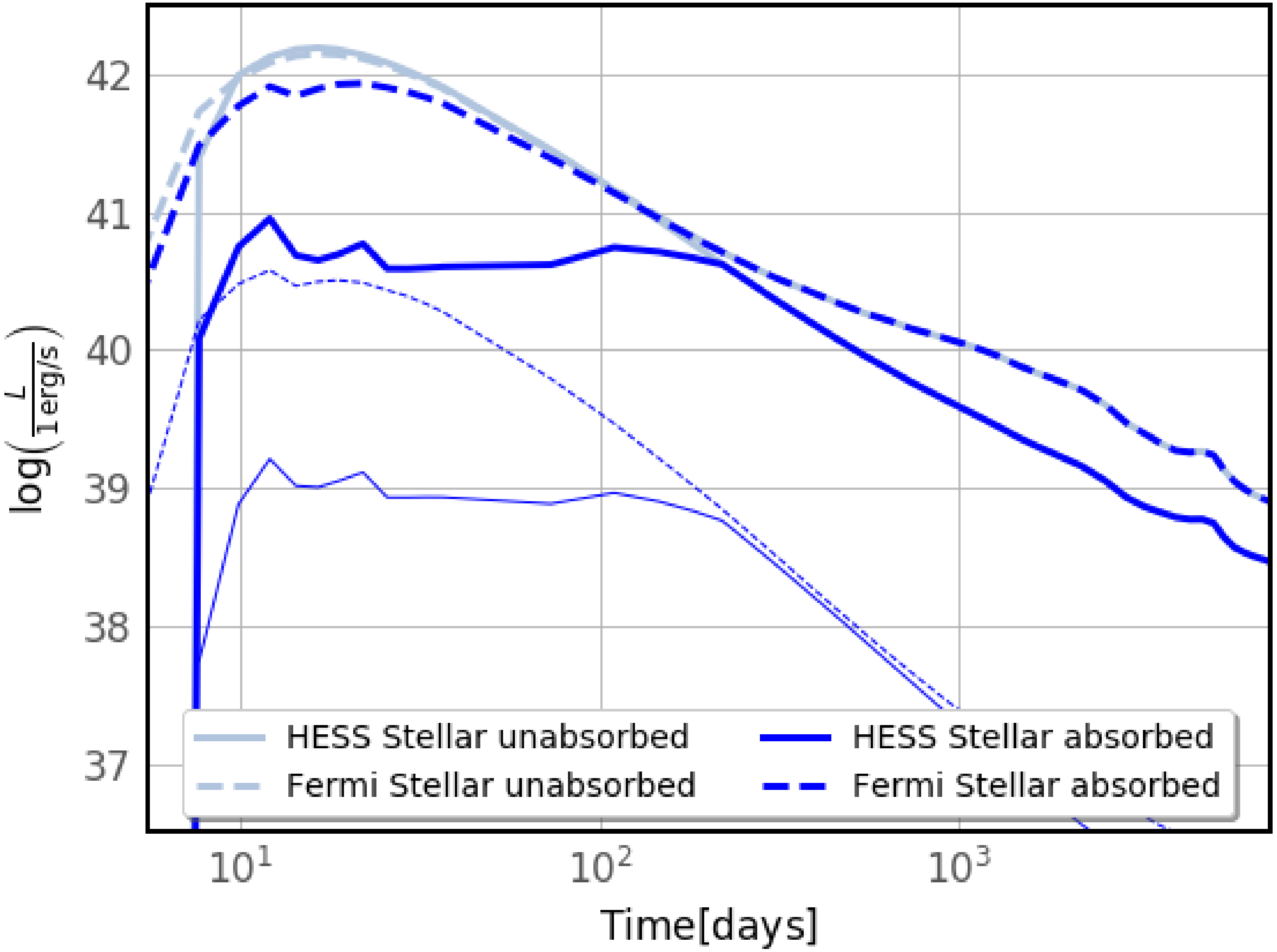

Gamma-ray emission

Time evolution of gamma-ray emission

- Peak-luminosity in HE gamma-rays after ~220days

- Peak-luminosity in VHE gamma-rays **5-10x above** steady-mass-loss case → **Lack of absorption;** reached after ~260days

- Fast-rising luminosities but ~40days shift between HE and VHE peaks

- Very-fast ($\propto t^{-4}$) decline after shock-shell interaction → short observational time-window

Figure: Gamma-ray luminosity over time.

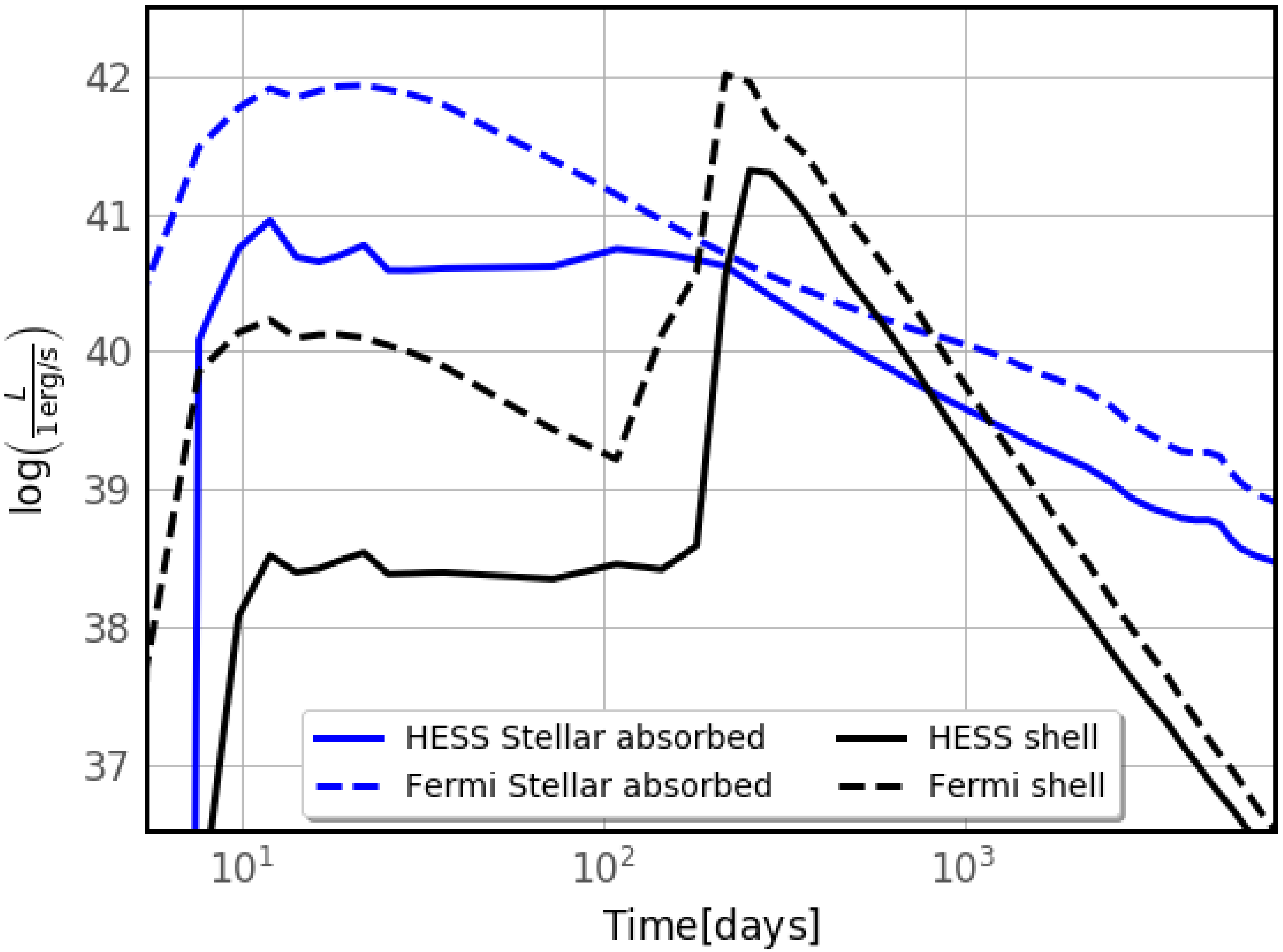

Non-thermal particle distribution

Radio emission

Smooth wind:

- Radio emission rise-times and peak-luminosities consistent with observations
- Injection-fraction based on historical remnants (e.g. SN1006) and magnetic field-amplification automatically produce the right radio-flux
- Strong spectral-index evolution due to free-free absorption

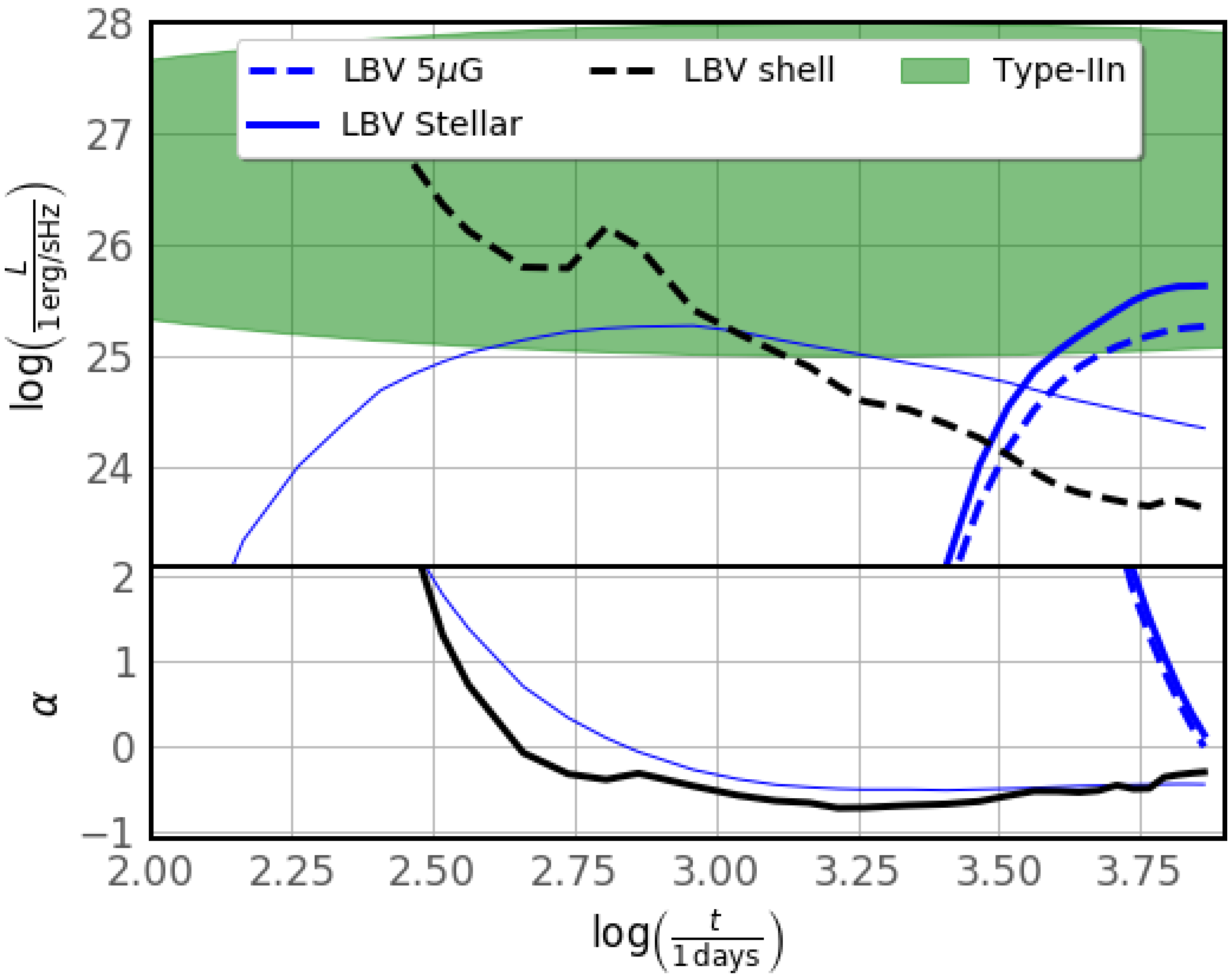

Figure(top): Radio luminosity at 8GHz.
Figure(right): Radio spectral-index 8GHz.

Non-thermal particle distribution
Radio emission

DIAS

Shell:

- Complete absorption when $R_{shock} < R_{shell}$
- First peak reached after ~300days
  → **peaks after gamma-ray emission**
- **Soft-radio index** due to shock-shell interaction
- **~10 times brighter** then in smooth wind

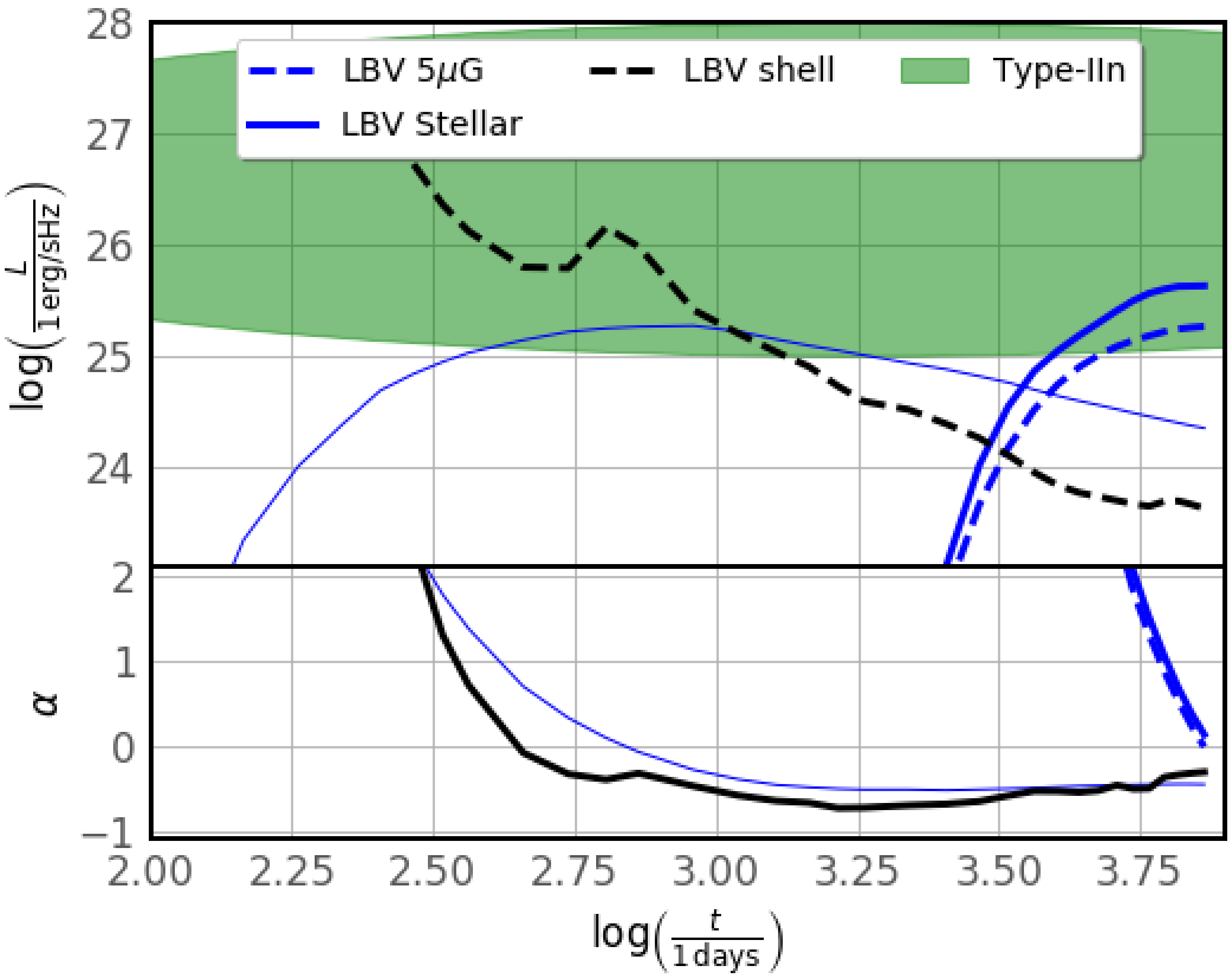

Figure(top): Radio luminosity at 8GHz.
Figure(right): Radio spectral-index 8GHz.

Conclusions and future work

- 1D time-dependent modelling of hydrodynamics, particle acceleration, magnetic-turbulence and high-energy radiation, from SN expanding into LBV (and RSG winds; see Brose et al 2022)

Smooth wind:

- **Unlikely to be PeVatrons**
- Detection horizon of ~3Mpc for LBVs
- Good agreement between observed and predicted Radio-emission

(see also Brose et al. 2022)

Shells:

- **Late-time re-brightening** at GeV, TeV gamma-rays, Radio and thermal X-rays
- Better detection-prospects due to reduced absorption in the VHE-domain → **5-10x brighter**
- Strong spectral index-evolution in the Radio due-to shell-interaction: hardening after shell-interaction (as observed in SN1987A)
- **Possibile PeVatrons → Closer shells = higher E_{max}**

Thank you for your attention!